View metadata, citation and similar papers at core.ac.uk
brought to you by CORE
provided by Sydney eScholarship

The first patient treatment of computed tomography ventilation functional image-guided radiotherapy for lung cancer

TokihiroYamamoto[a], SvenKabus[b], MatthieuBal[c], PaulKeall[d], StanleyBenedict[a], MeganDaly[a]

[a] Department of Radiation Oncology, University of California Davis School of Medicine, Sacramento, USA
[b] Department of Digital Imaging, Philips Research, Hamburg, Germany
[c] Philips Healthcare, Best, The Netherlands
[d] Radiation Physics Laboratory, Sydney Medical School, University of Sydney, Camperdown, Australia

Corresponding author:
Tokihiro Yamamoto
Department of Radiation Oncology, University of California Davis School of Medicine, 4501 X St., Sacramento, CA 9
toyamamoto@ucdavis.edu.au

Keywords

Lung cancer, Radiation pneumonitis, Lung functional imaging, 4D CT, Deformable image registration

Conflict of interest statement

Dr. Kabus and Dr. Bal are employees of Philips. Dr. Keall is an inventor of the issued patent, Method and system for using computed tomography to test pulmonary function (US 7668357).

Acknowledgments

This study was supported in part by the American Cancer Society and the Dean of the UC Davis School of Medicine (ACS IRG-95-125-13). Lihong Qi, Ph.D. in the Department of Public Health Sciences, Ken Yoneda, M.D. in the Department of Internal Medicine, and Friedrich Knollmann, M.D., Ph.D. in the Department of Radiology at UC Davis provided valuable contributions to the development of the clinical trial protocol. Satoshi Kida, Ph.D. at Tohoku University assisted in implementing the research objectives in Pinnacle. The authors thank Cari Wright in the Department of Radiation Oncology at UC Davis for serving as the primary treatment planner for this clinical trial. Philips Radiation Oncology Systems loaned us a research version of the Pinnacle3 treatment planning system.

Abstract

Background and purpose

Radiotherapy that selectively avoids irradiating highly-functional lung regions may reduce pulmonary toxicity. We report on the first clinical implementation and patient treatment of lung functional image-guided radiotherapy using an emerging technology, computed tomography (CT) ventilation imaging.

Material and methods

A protocol was developed to investigate the safety and feasibility of CT ventilation functional image-guided radiotherapy. CT ventilation imaging is based on (1) deformable image registration of four-dimensional (4D) CT images, and (2) quantitative image analysis for regional volume change, a surrogate for ventilation. CT ventilation functional image-guided radiotherapy plans were designed to minimize specific lung dose–function metrics, including functional V_{20} (fV_{20}), while maintaining target coverage and meeting standard constraints to other critical organs.

Results

CT ventilation functional image-guided treatment planning reduced the lung fV_{20} by 5% compared to an anatomic image-guided plan for an enrolled patient with stage IIIB non-small cell lung cancer. Although the doses to several other critical organs increased, the necessary constraints were all met.

Conclusions

An emerging technology, CT ventilation imaging has been translated into the clinic and used in functional image-guided radiotherapy for the first time. This milestone represents an important first step toward hypothetically reduced pulmonary toxicity in lung cancer radiotherapy.

Introduction

Pulmonary toxicity is substantial in lung cancer radiotherapy, particularly for locally advanced disease [1], [2]. Symptomatic (grade ⩾2) radiation pneumonitis is a common toxicity that occurs in approximately 30% of patients irradiated for lung cancer, with fatal pneumonitis in about 2% [1], [2]. The current paradigm of radiotherapy is based on anatomic imaging and assumes a homogeneous radiation dose–response of normal tissues. Radiotherapy that selectively avoids irradiating highly-functional lung regions may reduce pulmonary toxicity. This hypothesis is supported by several reports in the literature, demonstrating that lung dose–function metrics improve predictive power for pulmonary toxicity compared to dose–volume metrics (the current clinical standard) [3], [4]. For example, the functional V_{20} (fV_{20}) (percent lung function receiving ⩾20 Gy) was demonstrated to correlate more strongly with grade ⩾3 pneumonitis than the V_{20} (percent lung volume receiving ⩾20 Gy) [4]. Furthermore, information of regional lung function (e.g., defect) was found to be useful in predicting toxicity [5], [6], [7].

Several modalities exist for lung ventilation imaging [8], [9], [10], including an emerging method based on four-dimensional (4D) computed tomography (CT) and image processing/analysis [11], [12], henceforth referred to as CT ventilation imaging. CT ventilation imaging has a higher resolution, lower cost, shorter scan time, and/or greater availability, compared to other modalities, e.g., nuclear medicine and magnetic resonance (MR) imaging. Moreover, CT ventilation can be considered ‘free’ information in lung cancer radiotherapy, as 4D CT is currently in routine use at many centers and ventilation computation only involves image processing/analysis. Thus, CT ventilation imaging has a higher potential for widespread clinical implementation and would facilitate multi-institutional clinical trials as discussed in an editorial of a recent issue of Radiotherapy and Oncology [7]. The accuracy and reproducibility of CT ventilation imaging have been investigated extensively through animal studies [13], [14] and human studies [14], [15], [16], [17], [18]. Reasonable correlations with pulmonary function tests (PFTs) [17], [18] and other ventilation imaging modalities [13], [15], [17] indicate physiologic significance of CT ventilation imaging. See Appendix A for a full summary of the previous studies comparing CT ventilation with other modalities, most of which have demonstrated moderate to strong correlations.

Dosimetric significance of lung functional image-guided radiotherapy planning has been demonstrated by several investigators [19], [20], [21], [22], [23]. However, it is not known whether such dosimetric significance leads to clinical significance. Ultimately clinical trials are needed to test this hypothesis. In this paper, we describe the first clinical implementation and patient treatment of CT ventilation functional image-guided radiotherapy for lung cancer through a prospective clinical trial.

Materials and methods

Clinical trial protocol and patients

A protocol (NCT02308709) (details available upon request from the corresponding author) was developed for a prospective clinical trial to investigate the safety and feasibility of CT ventilation functional image-guided radiotherapy. The primary endpoint is any grade $\geqslant$3 adverse events defined as definitely, probably, or possibly related to the protocol treatment over the first 12 months of follow-up or drop-out due to intolerance of treatment. The necessary institutional review board and legal processes were completed prior to patient enrollment. The legal processes included an agreement between the Regents of the University of California (UC) and Philips Healthcare, providing software and hardware. We report implementation of CT ventilation functional image-guided radiotherapy in the first patients enrolled on this clinical trial, and provide dosimetric results of one enrolled patient with stage IIIB non-small cell lung cancer (NSCLC).

CT ventilation imaging

CT ventilation imaging is based on (1) deformable image registration (DIR) of 4D CT images, and (2) quantitative image analysis for regional volume change, a surrogate for ventilation. 4D CT scans were acquired using a Brilliance Big Bore multislice CT scanner (Philips Healthcare, Andover, MA). The respiratory signal was acquired using a pneumatic belt. The following standard 4D CT scan parameters were used: 120 kVp, 120 mA, and 2 mm slice thickness. DIR was performed for spatial mapping of the peak-inhalation 4D CT image (moving image) to the peak-exhalation image (fixed image). We employed a volumetric elastic DIR method that minimizes both a similarity function (sum of squared difference) and a regularization term (elastic regularization) [24]. The DIR method has been previously evaluated thoroughly [24], [25], [26] and demonstrated to achieve sub-voxel target registration errors on average [24]. Regional volume change was quantified using the Hounsfield unit (HU)-based metric. See Appendix B for further details on the HU-based metric.

CT ventilation functional image-guided radiotherapy

CT ventilation functional image-guided radiotherapy plans are designed to selectively avoid irradiating highly-functional lung regions and meet specific dose–function constraints, while maintaining target coverage and meeting standard constraints to other critical organs (Table 1). The lung dose–function constraints were determined based on Vinogradskiy et al. [4], and are estimated to yield a lower rate of radiation pneumonitis. Treatment is given 5 days per week for 30 days in 2 Gy fractions daily (60 Gy in total) using 6 MV photon beams for patients receiving

conventionally-fractionated radiotherapy with or without chemotherapy (concurrent chemotherapy for the patient reported in this paper). The same prescription dose and constraints to critical organs are used regardless of whether chemotherapy is used. Both intensity-modulated radiotherapy (IMRT) and volumetric modulated arc therapy (VMAT) are allowed.

The dose of 60 Gy was prescribed to 95% of the planning target volume (PTV). The minimum dose and maximum dose to the PTV must be $\geqslant$90% and $\leqslant$115% of the prescription dose, respectively. The gross tumor volume (GTV) was defined as the primary tumor and any regionally involved lymph nodes identified by treatment planning CT images (>1 cm on short axis). The internal target volume (ITV) was defined as the envelope that encompassed the GTV plus a full range of motion of the primary tumor and nodal target identified by 4D CT. A maximum intensity projection (MIP) image and peak-exhalation/inhalation 4D CT images were also used. The clinical target volume (CTV) was determined by adding a margin of 5–10 mm to the ITV at the discretion of the treating physician. The PTV was determined by adding an additional margin of 5 mm to the CTV.

Major critical organs were contoured as follows. The spinal cord was contoured as the bony limits of the spinal canal at least 10 cm cranial and caudal to the PTV. The heart along with the pericardial sac was contoured from its base to apex. The entire circumference of the esophagus including the outermost fatty adventitia was contoured at least 10 cm cranial and caudal to the PTV.

IMRT and VMAT optimization for CT ventilation functional image-guided radiotherapy is based on a non-uniform weight (importance) factor map of the lung generated from a ventilation image, which is incorporated into a cost function. The Pinnacle3 treatment planning system, research version 9.7 (Philips Radiation Oncology Systems, Fitchburg, WI) was used in the current implementation. The lung weight factor map was generated by converting CT ventilation images into percentile distribution images in a manner similar to Vinogradskiy et al. [4]. The following two types of lung dose–function objectives were developed: (1) maximum fV_x (percentage of ventilation receiving $\geqslant$x Gy), and (2) maximum functional mean lung dose (fMLD) (MLD weighted by regional ventilation). See Appendix C for further details on the lung weight factor map and IMRT/VMAT cost function. For IMRT, the beam angles are optimized manually to avoid passing through highly-functional lung regions.

Clinical process

The clinical processes included (1) CT ventilation computation, (2) CT ventilation functional image-guided treatment planning, (3) patient-specific quality assurance (QA), and (4) treatment delivery. First, CT ventilation computation was performed using a standalone research computer on which the software for DIR and ventilation computation is installed. Given that ventilation computation only involves image processing/analysis, this process could potentially be seamlessly integrated into a treatment planning system in a commercial application. Second, a functional image-guided treatment plan was created by an experienced dosimetrist, who was trained beforehand, using the resulting CT ventilation weight factor map on Pinnacle3, research version 9.7. IMRT with ten non-coplanar beams was used for the patient reported in this paper. Intensity modulation was performed using the direct machine parameter optimization (DMPO) algorithm, where the maximum number of multileaf collimator (MLC) segments was set at ten. For a comparison purpose, an anatomic image-guided plan was also created without using any prior knowledge of regional ventilation of the patient. The resulting functional image-guided plan was transferred to Pinnacle3, clinical version 9.10 for the final dose calculation and review. Third, patient-specific QA was performed through independent monitor unit (MU) calculation and measurement of absolute dose distributions. The results were evaluated based on the same criteria used for standard treatments at UC Davis. Lastly, treatment was delivered with daily kV cone-beam CT (CBCT) guidance.

Results

Fig. 1 shows a comparison between the CT ventilation functional image-guided IMRT plan and comparison anatomic image-guided plan of an enrolled patient with stage IIIB NSCLC. The dose to highly-functional lung regions including the right posterior and left anterior/medial regions was reduced with CT ventilation functional image guidance. The lung fV_{20} was reduced by 5% from 29.7% to 24.6%. The fMLD was almost identical, i.e., 18.3 Gy in the anatomic image-guided plan vs. 18.1 Gy in the functional image-guided plan. For the dose–volume metrics, the V_{20} was reduced by 4.4% from 32.8% to 28.3%, whereas the V_5 increased considerably by 10.6% from 79.7% to 90.3%. The MLD was almost identical, i.e., 18.9 Gy vs. 19.1 Gy, suggesting that the reduction in dose–function metrics were not attributed to overall reduction of the lung dose but rather selective avoidance of highly-functional regions. The anatomic image-guided plan created without using any prior knowledge of regional ventilation resulted in the lung V_{20} of 32.8% that was well below the limit (37%), and hence the plan was not further optimized to reduce the V_{20}. Using CT ventilation images, the fV_{20} of anatomic image-guided plan was calculated to be 29.7% that was just below the limit (30%). CT ventilation functional image-guided planning was performed to reduce the fV_{20}. For other structures, the PTV dose homogeneity was degraded with a higher maximum dose, i.e., 67.4 Gy (anatomic) vs. 69.0 Gy (functional). Also the maximum spinal cord dose and mean esophageal dose increased (cord, 44.4 Gy vs. 46.5 Gy; esophagus, 38.6 Gy vs. 40.0 Gy). However, the functional image-guided plan met all the target dose specifications and constraints to the critical organs, except for the

optional mean esophageal dose constraint of 34 Gy. The measurement of absolute dose distributions as part of the patient-specific QA process resulted in the γ passing rate (3%/3 mm) of 95%.

Discussion

This paper reports on the first patient treatment of CT ventilation functional image-guided radiotherapy for lung cancer. This represents the second clinical implementation of lung functional imaging in radiotherapy. Hyperpolarized ^{3}He MR ventilation imaging was the first modality implemented in radiotherapy in 2014 [27]. There are three major differences between these two implementations. First, CT ventilation imaging has a higher potential for widespread clinical implementation than hyperpolarized gas MR ventilation imaging. CT ventilation can be considered 'free' information in lung cancer radiotherapy, as 4D CT scans are currently in routine use at many radiotherapy centers and ventilation computation only involves image processing and analysis. Currently 4D CT is estimated to be used at approximately 70% of centers in the US, extrapolated from survey results by Simpson et al. [28]. CT ventilation imaging would also facilitate multi-institutional clinical trials as recently discussed by Ebert et al. [7]. By contrast, hyperpolarized ^{3}He MR ventilation imaging is limited by high costs, low availability, and poor global supply of ^{3}He gas. Second, CT ventilation images can be more easily registered to the planning CT image than MR ventilation images. Unlike MRI, 4D CT scans are usually acquired during the same session in the same position as the planning CT scans. The differences in the scan acquisition time, position, and breathing maneuver between MRI and planning CT make image registration difficult. Lastly, the voxel-based functional avoidance strategy was employed in the current implementation, whereas the sub-volume-based strategy was used in the hyperpolarized ^{3}He MR study. For dose painting, the voxel-based strategy (dose painting by numbers) was demonstrated to have dosimetric advantages over the sub-volume-based strategy (sub-volume boosting) [29].

The impact of lung functional image-guided treatment planning would vary with regional function, target size, location and delivery technique [20], [23]. Reductions in lung dose–function metrics may be greater for future patients to be enrolled in this trial than the patient described above. Lung functional avoidance is sometimes achieved at the expense of increased doses to other critical organs and/or degraded target dose homogeneity and conformity [21], [23] as observed for the patient reported in this paper. This raises a concern that lung functional image-guided radiotherapy might increase risk of non-pulmonary toxicity for some patients. Moreover, the lung volume receiving low doses for the patient reported in this paper was considerably larger in the functional image-guided plan (90.3%) than in the anatomic image-guided plan (79.7%). This raises a concern of pulmonary toxicity [30] as well, especially given that the $V_5 < 65\%$ is recommended by several investigators [2] and used as a constraint in several trials including RTOG 1106. Our trial does not include V_5 as a constraint, but rather V_{20} and

MLD in a manner similar to RTOG 0617. We will track various dose–volume metrics including those that are not used as a constraint, and assess any acute and late adverse events.

This ongoing clinical trial will enroll a total of 20 patients and analyze the rate of any grade $\geqslant 3$ adverse events over the first 12 months of follow-up or drop-out due to intolerance of treatment. The success of this study, i.e., a rate of grade $\geqslant 3$ adverse events less than 30% (derived from the published toxicity data) will provide a necessary justification for proceeding with a larger clinical trial (e.g., multi-institutional trial) to examine whether CT ventilation functional image-guided radiotherapy reduces pulmonary toxicity.

Clinical translational relevance

An emerging imaging technology, CT ventilation imaging has been translated into the clinic and used in functional image-guided radiotherapy for the first time. This milestone represents an important first step toward hypothetically reduced pulmonary toxicity in lung cancer radiotherapy and widespread implementation of CT ventilation imaging. Upon successful completion of this trial, we will conduct a larger clinical trial to examine the efficacy of CT ventilation functional image-guided radiotherapy.

Table 1. Dose–volume/function constraints to critical organs.

Critical organ	Constraint
Lung	V_{20} < 37%
	MLD < 20 Gy
	Functional V_{20} (fV_{20}) <30%
	Functional MLD (fMLD) <19 Gy
Spinal cord	Max dose < 47 Gy
Esophagus	Max dose < 70 Gy
	Mean dose <34 Gy[a]
Heart	Max dose < 70 Gy
	V_{60} < 33%
	V_{45} < 66%

Abbreviations: V_x = percent volume receiving $\geqslant x$ Gy, MLD = mean lung dose.

[a] Only a guideline and will not be scored as a protocol deviation if not achieved.

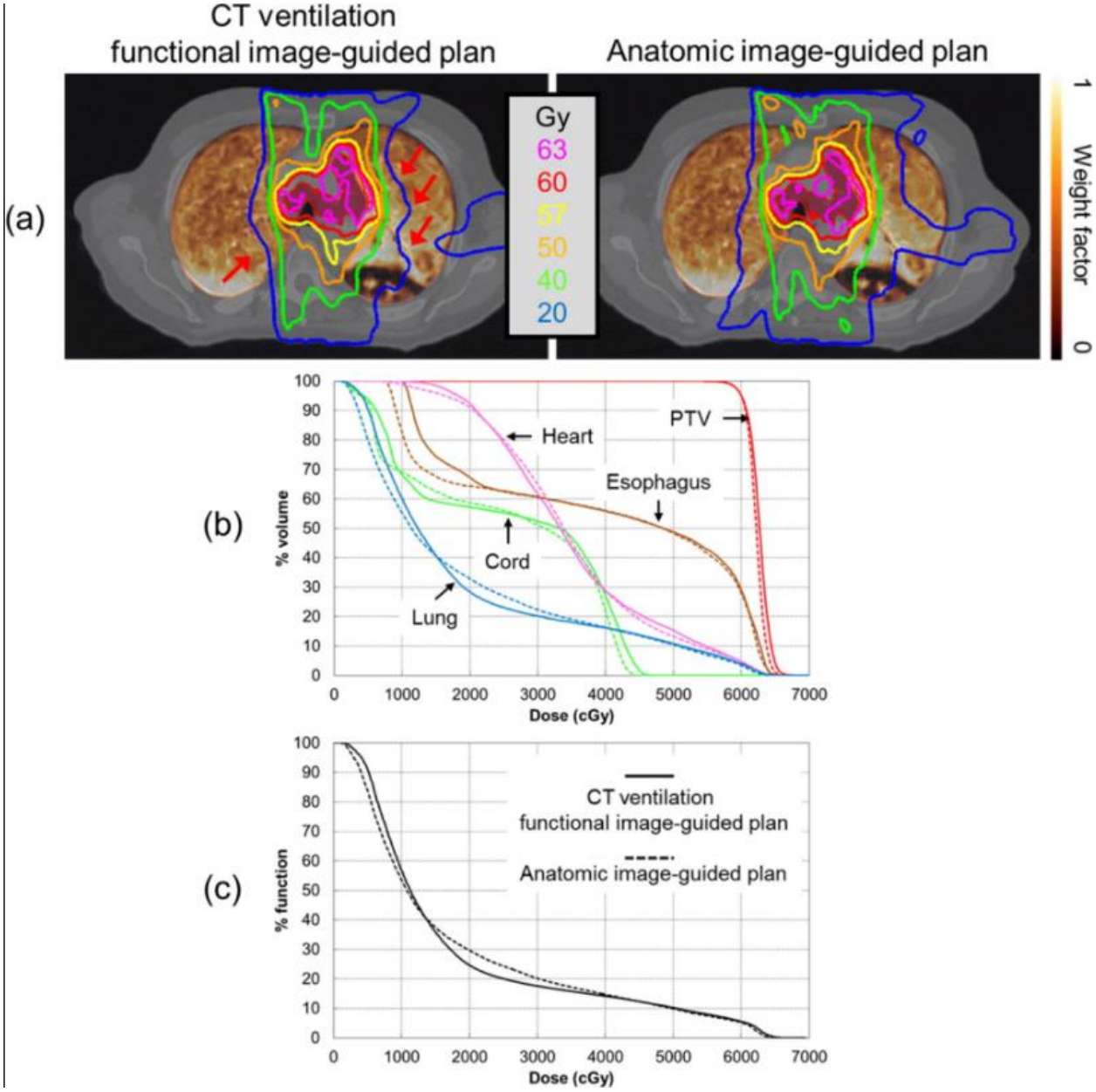

Fig. 1. Comparison of the CT ventilation functional image-guided IMRT plan and comparison anatomic image-guided plan: (a) isodose curves, (b) dose–volume histograms (DVHs) of the PTV (red) and critical organs (esophagus, brown; heart, purple; spinal cord, green; and lung, blue), and (c) lung dose–function histograms (DFHs) for an enrolled patient with stage IIIB NSCLC. The dose to highly-functional lung regions was reduced with functional image guidance (red arrows). A ventilation weight factor map is overlaid on the CT image. In the DVHs and DFHs, the solid and dashed lines denote the ventilation functional image-guided plan and anatomic image-guided plan, respectively.

[1] Palma DA, Senan S, Tsujino K, Barriger RB, Rengan R, Moreno M, et al. Predicting radiation pneumonitis after chemoradiation therapy for lung cancer: an international individual patient data meta-analysis. Int J Radiat Oncol Biol Phys 2013;85:444–50.

[2] Jiang ZQ, Yang K, Komaki R, Wei X, Tucker SL, Zhuang Y, et al. Long-term clinical outcome of intensity-modulated radiotherapy for inoperable nonsmall cell lung cancer: the MD Anderson experience. Int J Radiat Oncol Biol Phys 2012;83:332–9.

[3] Seppenwoolde Y, De Jaeger K, Boersma LJ, Belderbos JS, Lebesque JV. Regional differences in lung radiosensitivity after radiotherapy for non-small-cell lung cancer. Int J Radiat Oncol Biol Phys 2004;60:748–58.

[4] Vinogradskiy Y, Castillo R, Castillo E, Tucker SL, Liao Z, Guerrero T, et al. Use of 4-dimensional computed tomography-based ventilation imaging to correlate lung dose and function with clinical outcomes. Int J Radiat Oncol Biol Phys 2013;86:366–71.

[5] Abratt RP, Willcox PA, Smith JA. Lung cancer in patients with borderline lung functions-zonal lung perfusion scans at presentation and lung function after high dose irradiation. Radiother Oncol 1990;19:317–22.

[6] Gayed IW, Chang J, Kim EE, Nunez R, Chasen B, Liu HH, et al. Lung perfusion imaging can risk stratify lung cancer patients for the development of pulmonary complications after chemoradiation. J Thorac Oncol 2008;3: 858–64.

[7] Ebert N, Baumann M, Troost EG. Radiation-induced lung damage – clinical risk profiles and predictive imaging on their way to risk-adapted individualized treatment planning? Radiother Oncol 2015;117:1–3.

[8] Petersson J, Sanchez-Crespo A, Larsson SA, Mure M. Physiological imaging of the lung: single-photon-emission computed tomography (SPECT). J Appl Physiol 2007;102:468–76.

[9] van Beek EJ, Wild JM, Kauczor HU, Schreiber W, Mugler 3rd JP, de Lange EE. Functional MRI of the lung using hyperpolarized 3-helium gas. J Magn Reson Imaging 2004;20:540–54.

[10] Chae EJ, Seo JB, Goo HW, Kim N, Song KS, Lee SD, et al. Xenon ventilation CT with a dual-energy technique of dual-source CT: initial experience. Radiology 2008;248:615–24.

[11] Guerrero T, Sanders K, Noyola-Martinez J, Castillo E, Zhang Y, Tapia R, et al. Quantification of regional ventilation from treatment planning CT. Int J Radiat Oncol Biol Phys 2005;62:630–4.

[12] Guerrero T, Sanders K, Castillo E, Zhang Y, Bidaut L, Pan T, et al. Dynamic ventilation imaging from four-dimensional computed tomography. Phys Med Biol 2006;51:777–91.

[13] Reinhardt JM, Ding K, Cao K, Christensen GE, Hoffman EA, Bodas SV. Registration-based estimates of local lung tissue expansion compared to xenon CT measures of specific ventilation. Med Image Anal 2008;12:752–63.

[14] Du K, Bayouth JE, Cao K, Christensen GE, Ding K, Reinhardt JM. Reproducibility of registration-based measures of lung tissue expansion. Med Phys 2012;39:1595–608.

[15] Mathew L, Wheatley A, Castillo R, Castillo E, Rodrigues G, Guerrero T, et al. Hyperpolarized (3)He magnetic resonance imaging: comparison with fourdimensional X-ray computed tomography imaging in lung cancer. Acad Radiol 2012;19:1546–53.

[16] Yamamoto T, Kabus S, von Berg J, Lorenz C, Chung MP, Hong JC, et al. Reproducibility of four-dimensional computed tomography-based lung ventilation imaging. Acad Radiol 2012;19:1554–65.

[17] Yamamoto T, Kabus S, Lorenz C, Mittra E, Hong JC, Chung M, et al. Pulmonary ventilation imaging based on 4-dimensional computed tomography: comparison with pulmonary function tests and SPECT ventilation images. Int J Radiat Oncol Biol Phys 2014;90:414–22.

[18] Brennan D, Schubert L, Diot Q, Castillo R, Castillo E, Guerrero T, et al. Clinical validation of 4-dimensional computed tomography ventilation with pulmonary function test data. Int J Radiat Oncol Biol Phys 2015;92:423–9.

[19] Marks LB, Spencer DP, Sherouse GW, Bentel G, Clough R, Vann K, et al. The role of three dimensional functional lung imaging in radiation treatment planning: the functional dose–volume histogram. Int J Radiat Oncol Biol Phys 1995;33:65–75.

[20] Seppenwoolde Y, Engelsman M, De Jaeger K, Muller SH, Baas P, McShan DL, et al. Optimizing radiation treatment plans for lung cancer using lung perfusion information. Radiother Oncol 2002;63:165–77.

[21] Ireland RH, Bragg CM, McJury M, Woodhouse N, Fichele S, van Beek EJ, et al. Feasibility of image registration and intensity-modulated radiotherapy planning with hyperpolarized helium-3 magnetic resonance imaging for non-small-cell lung cancer. Int J Radiat Oncol Biol Phys 2007;68:273–81.

[22] Bates EL, Bragg CM, Wild JM, Hatton MQ, Ireland RH. Functional image-based radiotherapy planning for non-small cell lung cancer: a simulation study. Radiother Oncol 2009;93:32–6.

[23] Yamamoto T, Kabus S, von Berg J, Lorenz C, Keall PJ. Impact of fourdimensional computed tomography pulmonary ventilation imaging-based functional avoidance for lung cancer radiotherapy. Int J Radiat Oncol Biol Phys 2011;79:279–88.

[24] Kabus S, Lorenz C. Fast elastic image registration. Proc of the Medical Image Analysis For The Clinic – A grand challenge. MICCAI 2010:81–9.

[25] Kabus S, Klinder T, Murphy K, van Ginneken B, Lorenz C, Pluim JPW. Evaluation of 4D-CT Lung Registration. In: Yang GZ, Hawkes DJ, Rueckert D, Noble JA, Taylor CJ, editors. Proc of MICCAI:London, UK, 2009. p. 747–54.

[26] Murphy K, van Ginneken B, Reinhardt JM, Kabus S, Ding K, Deng X, et al. Evaluation of registration methods on thoracic CT: the EMPIRE10 challenge. IEEE Trans Med Imaging 2011;30:1901–20.

[27] Hoover DA, Capaldi DP, Sheikh K, Palma DA, Rodrigues GB, Dar AR, et al. Functional lung avoidance for individualized radiotherapy (FLAIR): study protocol for a randomized, double-blind clinical trial. BMC Cancer 2014;14:934.

[28] Simpson DR, Lawson JD, Nath SK, Rose BS, Mundt AJ, Mell LK. Utilization of advanced imaging technologies for target delineation in radiation oncology. J Am Coll Radiol 2009;6:876–83.

[29] Vanderstraeten B, Duthoy W, De Gersem W, De Neve W, Thierens H. [18F] fluoro-deoxy-glucose positron emission tomography ([18F]FDG-PET) voxel intensity-based intensity-modulated radiation therapy (IMRT) for head and neck cancer. Radiother Oncol 2006;79:249–58.

[30] Wang S, Liao Z, Wei X, Liu HH, Tucker SL, Hu CS, et al. Analysis of clinical and dosimetric factors associated with treatment-related pneumonitis (TRP) in patients with non-small-cell lung cancer (NSCLC) treated with concurrent chemotherapy and three-dimensional conformal radiotherapy (3D-CRT). Int J Radiat Oncol Biol Phys 2006;66:1399–407.

Appendix A: Summary of the previous studies comparing CT ventilation imaging with other modalities

Study	Modality	Subjects	Key finding
Yamamoto *et al*. [1]	PFT	15 human subjects	Moderate correlations (range 0.43-0.73) between CT ventilation-defined defect parameters and PFT parameters
Brennan *et al*. [2]	PFT	98 human subjects	Moderate correlations (range 0.63-0.72) between CT ventilation-defined parameters (heterogeneity and defect) and PFT parameters
Fuld *et al*. [3]	Xenon-CT	4 sheep	Strong correlation (0.81) of regional ventilation
Reinhardt *et al.* [4]	Xenon-CT	5 sheep	Strong correlation (0.85) of regional ventilation
Mathew *et al*. [5]	Hyperpolarized ^{3}He MRI	11 human subjects	Strong DSCs (0.86-0.88) of ventilated volumes
Vinogradskiy *et al*. [6]	^{99m}Tc-DTPA scintigraphy	15 human subjects	Moderate correlation (0.68) of % ventilation of each lung
Castillo *et al*. [7]	^{99m}Tc-DTPA SPECT	7 human subjects	Weak DSC (0.35) of poorly-ventilated volumes likely due to central airway deposition of aerosols
Yamamoto *et al*. [1]	^{99m}Tc-DTPA SPECT	16 human subjects	Significantly lower CT ventilation in SPECT-defined defect regions than in non-defect regions
Kipritidis *et al*. [8]	^{68}Ga-aerosol (Galligas) PET	12 human subjects	Strong DSC (0.88) of ventilated volumes; moderate DSC (0.52) of poorly-ventilated volumes; moderate (0.42) correlation of regional ventilation

Abbreviations: PFT = pulmonary function test, ^{99m}Tc-DTPA = technetium-99m-labeled diethylenetriamine pentaacetate, DSC = Dice similarity coefficient.

[1] Yamamoto T, Kabus S, Lorenz C, Mittra E, Hong JC, Chung M, et al. Pulmonary Ventilation Imaging Based on 4-Dimensional Computed Tomography: Comparison With Pulmonary Function Tests and SPECT Ventilation Images. Int J Radiat Oncol Biol Phys. 2014;90:414-22.

[2] Brennan D, Schubert L, Diot Q, Castillo R, Castillo E, Guerrero T, et al. Clinical validation of 4-dimensional computed tomography ventilation with pulmonary function test data. Int J Radiat Oncol Biol Phys. 2015;92:423-9.

[3] Fuld MK, Easley RB, Saba OI, Chon D, Reinhardt JM, Hoffman EA, et al. CT-measured regional specific volume change reflects regional ventilation in supine sheep. J Appl Physiol. 2008;104:1177-84.

[4] Reinhardt JM, Ding K, Cao K, Christensen GE, Hoffman EA, Bodas SV. Registration-based estimates of local lung tissue expansion compared to xenon CT measures of specific ventilation. Med Image Anal. 2008;12:752-63.

[5] Mathew L, Wheatley A, Castillo R, Castillo E, Rodrigues G, Guerrero T, et al. Hyperpolarized (3)He magnetic resonance imaging: comparison with four-dimensional x-ray computed tomography imaging in lung cancer. Acad Radiol. 2012;19:1546-53.

[6] Vinogradskiy Y, Koo PJ, Castillo R, Castillo E, Guerrero T, Gaspar LE, et al. Comparison of 4-dimensional computed tomography ventilation with nuclear medicine ventilation-perfusion imaging: a clinical validation study. Int J Radiat Oncol Biol Phys. 2014;89:199-205.

[7] Castillo R, Castillo E, Martinez J, Guerrero T. Ventilation from four-dimensional computed tomography: density versus Jacobian methods. Phys Med Biol. 2010;55:4661-85.

[8] Kipritidis J, Siva S, Hofman MS, Callahan J, Hicks RJ, Keall PJ. Validating and improving CT ventilation imaging by correlating with ventilation 4D-PET/CT using (68)Ga-labeled nanoparticles. Med Phys. 2014;41:011910.

Appendix B: Derivation of the Hounsfield unit-based ventilation metric

Simon [1] derived a relationship between the regional change in fractional air content and regional volume change, which was adapted to the relationship between the local Hounsfield unit (HU) change and local volume change by Guerrero *et al.* [2]. The specific ventilation in the voxel at location (x, y, z) is given by

$$\frac{\Delta \mathrm{Vol}}{\mathrm{Vol}_{\mathrm{ex}}^{\mathrm{air}}(x,y,z)} = 1000 \frac{\mathrm{HU}_{\mathrm{in}}\{x+u_x(x,y,z), y+u_y(x,y,z), z+u_z(x,y,z)\} - \mathrm{HU}_{\mathrm{ex}}(x,y,z)}{\mathrm{HU}_{\mathrm{ex}}(x,y,z)\left[\mathrm{HU}_{\mathrm{in}}\{x+u_x(x,y,z), y+u_y(x,y,z), z+u_z(x,y,z)\}+1000\right]}, \quad (1)$$

where HU is the HU value and u is the displacement vector mapping the voxel at location (x, y, z) of a peak-exhalation 4D-CT image to the corresponding location of a peak-inhalation image. $\mathrm{HU}_{\mathrm{in}}$ represents the peak-inhalation HU value after correction for the lung mass variation from the peak-exhalation phase (see below). Note that the air and tissue densities were assumed to be -1000 and 0 HU, respectively. The peak-exhalation air volume ($\mathrm{Vol}_{\mathrm{ex}}^{\mathrm{air}}$) in the voxel at location (x, y, z) can be estimated by

$$\mathrm{Vol}_{\mathrm{ex}}^{\mathrm{air}}(x,y,z) = -\frac{\mathrm{HU}_{\mathrm{ex}}(x,y,z)}{1000}\mathrm{Vol}_{\mathrm{ex}}^{\mathrm{voxel}}(x,y,z), \quad (2)$$

where $\mathrm{Vol}_{\mathrm{ex}}^{\mathrm{voxel}}$ is the peak-exhalation voxel volume [3]. Substitution of Equation (2) into Equation (1) yields

$$\Delta \mathrm{Vol} = \frac{\mathrm{HU}_{\mathrm{ex}}(x,y,z) - \mathrm{HU}_{\mathrm{in}}\{x+u_x(x,y,z), y+u_y(x,y,z), z+u_z(x,y,z)\}}{\mathrm{HU}_{\mathrm{in}}\{x+u_x(x,y,z), y+u_y(x,y,z), z+u_z(x,y,z)\}+1000}\mathrm{Vol}_{\mathrm{ex}}^{\mathrm{voxel}}(x,y,z). \quad (3)$$

Given that $\mathrm{Vol}_{\mathrm{ex}}^{\mathrm{voxel}}$ is identical for all voxels, the HU-based ventilation metric ($V_{\mathrm{4DCT}}^{\mathrm{HU}}$) was defined as:

$$V_{\mathrm{4DCT}}^{\mathrm{HU}}(x,y,z) = \frac{\mathrm{HU}_{\mathrm{ex}}(x,y,z) - \mathrm{HU}_{\mathrm{in}}\{x+u_x(x,y,z), y+u_y(x,y,z), z+u_z(x,y,z)\}}{\mathrm{HU}_{\mathrm{in}}\{x+u_x(x,y,z), y+u_y(x,y,z), z+u_z(x,y,z)\}+1000} \cdot \rho_{\mathrm{scaling}}. \quad (4)$$

where ρ_{scaling} is the CT density scaling factor $\rho_{\mathrm{scaling}} = (\mathrm{HU}_{\mathrm{ex}} + 1024)/774$, which takes a value ranging from 0 for the voxel with the lowest lung CT density (-1024 HU) to 1 for the voxel with the highest density (-250 HU) [4, 5]. The rationale for density scaling is to transform a purely mechanical model of regional ventilation based on volume change alone to a more physiological model. Gas transport to high alveolar density regions contributes more to gas exchange, and hence is considered more physiologically relevant compared to gas transport to low alveolar density regions. It was assumed that alveolar density was proportional to CT density.

The peak-inhalation HU values were corrected for the lung mass variation from the peak-exhalation phase in the same manner as Guerrero *et al*. [6] by

$$\mathrm{HU}_{\mathrm{in}}^{\mathrm{corrected}} = \mathrm{HU}_{\mathrm{in}}^{\mathrm{uncorrected}} - 1000 f\left(1 + \frac{\mathrm{HU}_{\mathrm{in}}^{\mathrm{uncorrected}}}{1000}\right), \quad (5)$$

where f denotes the fractional difference in the lung mass between the peak-exhalation and peak-inhalation phases. Lung perfusion increases with inhalation due to several factors including distension of blood vessels and variation in cardiac output, leading to increased lung mass [6, 7].

[1] Simon BA. Non-invasive imaging of regional lung function using x-ray computed tomography. J Clin Monit Comput. 2000;16:433-42.
[2] Guerrero T, Sanders K, Noyola-Martinez J, Castillo E, Zhang Y, Tapia R, et al. Quantification of regional ventilation from treatment planning CT. Int J Radiat Oncol Biol Phys. 2005;62:630-4.

[3] Hoffman EA, Ritman EL. Effect of body orientation on regional lung expansion in dog and sloth. Journal of applied physiology. 1985;59:481-91.
[4] Kipritidis J, Siva S, Hofman MS, Callahan J, Hicks RJ, Keall PJ. Validating and improving CT ventilation imaging by correlating with ventilation 4D-PET/CT using (68)Ga-labeled nanoparticles. Med Phys. 2014;41:011910.
[5] Yamamoto T, Kabus S, Lorenz C, Mittra E, Hong JC, Chung M, et al. Pulmonary Ventilation Imaging Based on 4-Dimensional Computed Tomography: Comparison With Pulmonary Function Tests and SPECT Ventilation Images. Int J Radiat Oncol Biol Phys. 2014;90:414-22.
[6] Guerrero T, Sanders K, Castillo E, Zhang Y, Bidaut L, Pan T, et al. Dynamic ventilation imaging from four-dimensional computed tomography. Phys Med Biol. 2006;51:777-91.
[7] Brower R, Wise RA, Hassapoyannes C, Bromberger-Barnea B, Permutt S. Effect of lung inflation on lung blood volume and pulmonary venous flow. J Appl Physiol (1985). 1985;58:954-63.

Appendix C: Cost function for CT ventilation functional image-guided IMRT/VMAT optimization

Optimization is based on minimization of a cost function that is proportional to the sum of the objectives times the weight factors. A cost function Φ for CT ventilation functional image-guided IMRT/VMAT optimization is expressed as

$$\Phi \propto \sum_{k=1}^{N}\sum_{c=1}^{M}\phi\left(c, D_k, w_k\right)\cdot\eta_c, \qquad (1)$$

where N is the number of voxels in the lung, M is the number of lung dose-function objectives, ϕ is a function of the lung dose-function objective c, dose D_k deposited in the voxel k, and regional weight factor w_k of the voxel k, and η_c is the global weight factor assigned to the objective c. The regional weight factor w_k was determined as follows. CT ventilation images were converted into percentile distribution images by replacing the ventilation value of each voxel with the corresponding cumulative distribution function (CDF_k) scaled to the range [0, 1] in a manner similar to Vinogradskiy *et al*. [1]. When the ventilation value of the voxel k is denoted by V_k, the regional weight factor, w_k is given by

$$w_k = CDF_k = \frac{N_k \in [0, V_k]}{N}, \qquad (2)$$

where N_k is the number of voxels with a ventilation value in the range of $[0, V_k]$. The following two types of lung dose-function objectives were developed: (1) maximum fV_x (percentage of total CDF_k receiving ≥x Gy), and (2) maximum functional mean lung dose (fMLD) (MLD weighted by CDF_k).

[1] Vinogradskiy Y, Castillo R, Castillo E, Tucker SL, Liao Z, Guerrero T, et al. Use of 4-dimensional computed tomography-based ventilation imaging to correlate lung dose and function with clinical outcomes. Int J Radiat Oncol Biol Phys. 2013;86:366-71.